Simulation of Production Processes using the Multiphysics Approach: The Electrochemical Machining Process

R. van Tijum[*,1] and P.T. Pajak[1]
[1]Philips Consumer Lifestyle, Advanced Technology Center
*Corresponding author: Tussendiepen 4, P.O. Box 20100, 9200 CA Drachten, The Netherlands, redmer.van.tijum@philips.com

Abstract: The electric shaver is one of the successful products of Philips. One of the reasons of the superior shaving performance is the accuracy of the functional part of the shaver made from TRIP steel. The production process of this part consists of cold forming, heat treatment and finishing. The last step assures final product accuracy and thus enables required shaving performance. Electrochemical Machining process (ECM) is used as the finishing technological operation, which additionally enables accurate 3d shape freedom.

The aim of this paper is to explain complexity of the interactions involved in the ECM process. This is done experimentally using laboratory set-up – a flow channel cell that resembles production process and by modeling in COMSOL Multiphysics where a validated model is created. The last part of the paper shows how COMSOL simulation is applied to support design of ECM process of the shaving cap.

Keywords: Electrochemical Machining (ECM), validation, flow channel cell.

1. Introduction

Electrochemical machining (ECM) is an unconventional electrochemical process [1]. Gusseff patented the first controlled ECM process in 1929 [2] and the process was developed further by Jacquet in 1935 [3]. However, the principles of the process were invented by Faraday in 1833. After the Second World War, the technique became more common due to demanding processing of hard alloys by military and aerospace applications. Nowadays, ECM is well established in niche applications like turbine blades, medical implants and shaving heads [4,5].

ECM removes material at the anode (workpiece) using current controlled electrochemical process. By feeding a shaped cathode (tool or electrode) towards the workpiece, the reverse shape of the tool is copied to the workpiece. ECM can only take place if sufficient electrically conductive fluid (electrolyte) flow is maintained in the inter electrode gap. Typical a DC voltage up to 25 V is applied across the work piece and tool. Theoretical material removal rate is described by Faraday's law:

$$\frac{\Delta m}{\Delta t} = \frac{M \cdot I}{z \cdot F}, \qquad (1)$$

where: $\Delta m/\Delta t$ is the mass removal rate, M is the atomic weight, I is the current, z is the valance of the dissolved metal and F is the Faraday constant. The mass removal rate can be controlled by the current, process duration and depends on the workpiece material properties. In practice, the electrolyte type and potential drop in the gap will affect the mass removal rate. The electrolyte typically used are aqueous solutions of salts (e.g. NaCl, $NaNO_3$) or diluted acids [6,7].

ECM is applied by Philips Consumer Lifestyle for the mass scale production of the key functional part of the Philips shaving head. The production process of this part consists of cold forming, heat treatment and finishing. The last step is the ECM process that enables to achieve desired accuracy and thereby required shaving performance.

ECM is a complicated process incorporating number of phenomena interacting with each other. For example, any disturbance in the electrolyte flow regime can lead to a pressure drop and insufficient flushing (chocking) which may in turn in local electrolyte boiling (dead zone) and disturbance of dissolution negatively affecting machining accuracy. Figure 1 shows several typical problems in ECM related to electrolyte [1].

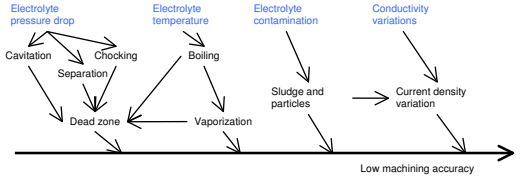

Figure 1. Simplified Ishikawa's diagram of the main electrolyte flow related problems in ECM [1].

Other common ECM problems are related to the variations of the material composition and the workpiece positioning. All the abovementioned process drawbacks can be minimized or avoided in the early process design stage using process simulation, which is of the key importance for the mass production in order to minimize process research and process design costs. This paper describes a part of the research performed at Philips Advanced Technology Center aimed to increase predictability and efficiency of the Philips shaving head finishing process.

2. Process background

In ECM, the velocity of the removed material v_n depends on current density J, material properties K and dissolution efficiency η (equation 2). Typically, high currents (>100A) are used to drive the process [1] and as a stray effect Joule heat is generated in the gap. Electrolyte flow not only enables to remove dissolved metal ions but assists to remove excessive heat by convection preventing electrolyte from boiling.

$$v_n = K \cdot \eta(J) \cdot J \,, \qquad (2)$$

In ECM with passivating electrolytes, chemical reactions occurring at each electrode depend on current density. Possible reactions at the anode include water oxidation (taking place likely at low current density) (equation 3) and material dissolution (equation 4). At the cathode hydrogen gas can be generated (equation 5). Moreover, metal ions can form hydroxides and nitrate reduction reactions can occur.

$$2H_2O \rightarrow O_2 + 4H^+ + 4e \qquad (3)$$

$$Me \leftrightarrow Me^{n+} + n \cdot e^- \qquad (4)$$

$$2 \cdot e^- + 2 \cdot H_2O \leftrightarrow H_2 + 2(OH^-) \qquad (5)$$

Gas generation in the process is inevitable and it adversely influences electrolyte conductivity. At the other hand, electrolyte is heated up by Joule heat that increases its conductivity. The process is stable when sufficient flushing is maintained – gas bubbles are flushed away and heat dissipated.

The process efficiency is determined by the likelihood of chemical reaction taking place in the system. In practice, however, process efficiency depends mainly on the current density, electrolyte and material properties of the workpiece. Process efficiency depends therefore on the process variables [8] that can be measured using flow channel cell set-up and can be described as follows (equation 6):

$$\eta(J) = c_1 + \frac{2}{\pi}(c_2 - c_1) \cdot \mathrm{atan}(c_3(J - c_4)) \,, \qquad (6)$$

where: c_1, c_2, c_3, c_4, constants describing the efficiency of the process.

The efficiency measurement is based on comparison of the theoretically calculated sample mass change in experiment compared to the actual experimental mass change.

3. Experimental setup

A laboratory ECM process investigation set-up – the flow channel cell is used to develop process simulation model (figure 2). The major advantage of the flow channel cell comparing to the production process is well-developed flow profile that simplifies simulation case.

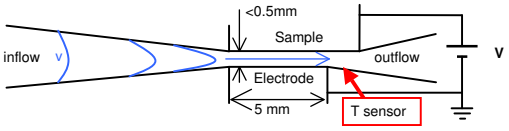

Figure 2. Flow channel cell diagram.

Electrolyte enters the channel at a certain pressure and its length is sufficient to achieve fully developed parabolic flow profile in the narrowest region. The average flow velocity in the gap is v_{max} = 28 m/s. Figure 2 schematically shows flow channel cell configuration. The top part is the sample (anode) and the bottom part is an electrode (cathode). The electrode length is 5 mm and the width is 7 mm. Behind the process gap electrolyte temperature and pH are measured. The sample is weighted before and after the experiment and its profile is measured after the experiment that describes the material removal along the sample.

4. Numerical model

The ECM model comprises several physical domains: Navier-Stokes flow description, electric field distribution, heat conduction & convection, gas convection and moving boundaries (workpiece material removal). All constitute a multiphysics problem.

Figure 3 shows the interactions which take place in the process. Electrolyte flow and electric current are driven by pressure and potential gradients, respectively. The electrolyte flow is

described by weakly compressible Navier-Stokes model taking into account 0.05 artificial diffusion. Joule heat and gas generated during the process determine conductivity of the electrolyte. Heat and gas are removed by conduction and convection and convection and diffusion, respectively. Current density distribution is calculated as a result of above interactions and it drives material removal (equation 2 see up).

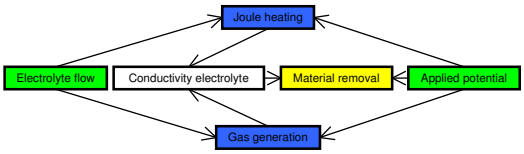

Figure 3. Schematic representation of the relationships between the different phenomena: (green) steering parameters, (blue) effect of steering, (white) indirect effect of steering and (yellow) the final material removal.

Simplified process relationships are shown in figure 3 and can be summarized by the equations of gas volume fraction in the electrolyte (equation 7) that with contribution of temperature determine conductivity of the electrolyte (equation 8).

$$volfrac = \frac{C}{C + M_{el}} \tag{7}$$

$$\frac{1}{\sigma} = \rho_0 (1 + volfrac)^{bp} \cdot (1 + \alpha (T - T_0)) \tag{8}$$

where: *volfrac* is gas volume fraction, C is gas concentration variable, M_{el} is electrolyte molar concentration, σ is electric conductivity, ρ_0 is resistivity at T_0, T_0 is the reference temperature, T is temperature variables, α is conductivity increase coefficient and *bp* is Brugeman's coefficient.

The amount of gas generated during the process expressed by gas fluxes is described at each electrode by equation 9.

$$N_{0,\text{electrode}} = \frac{J \cdot \eta(J)}{2F}$$
$$N_{0,\text{workpiece}} = \frac{J \cdot (1 - \eta(J))}{4F} \tag{9}$$

Here, N_0 is the gas flux, F the Faraday constant, J is current density and η is the process current efficiency. All the physic domains are hyperlinked by variables being solved simultaneously.

5. Experimental results

In order to build up ECM simulation model (Figure 3), at first process current efficiency behavior needs to be parameterized. This required carrying out experiments using flow channel cell set-up. Knowing physical principles and physical reactions determining current efficiency [9, 10], a set of experiments for three levels of inlet electrolyte temperature and for three electrolyte concentrations was performed. The experimental results are shown in Figure 4.

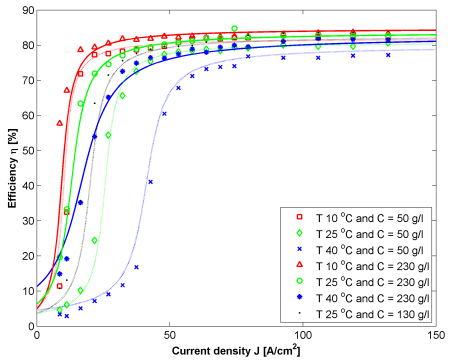

Figure 4. Current efficiency of the ECM process using passivating electrolyte as function of the current density J.

For low current densities, process current efficiency is relatively low due to dominance of water oxidation and oxygen evolution over the material dissolution reaction. For higher current densities current efficiency increases to a plateau of 80% and dissolution reaction prevails. High current efficiency also enables achievement of glossy surface finish. Increase of electrolyte concentration makes more active electrolyte ions available to take part in the electrochemical reactions and thus increases current efficiency. Transport of ions in ECM is a diffusion driven process, therefore according to Arhenius' Law, higher temperature intensifies that process. Taking into account theory of the diffusion salt layer in ECM [9, 10] that promotes material dissolution, higher temperature enhances diffusion and thus decreases current efficiency. For higher concentrations, the effect of temperature is less pronounced because more electrolyte ions are available to rebuild surface layer being diffused.

For each group of result points a data fit was made according to equation 6 resulting in a set of parameters. Combining all the curves, each parameter can be defined as a function of temperature T (°C) and concentration C (g/l):

$$\eta(J) = c_1 + \frac{2}{\pi}(c_2 - c_1)\cdot \mathrm{atan}(c_3(J - c_4))$$

$$c_1 = 40.7$$

$$c_2 = 75.4 - 0.0676\cdot T + 1.86\cdot \ln(C) \qquad (10)$$

$$c_3 = 0.684 - 0.00772\cdot T - 0.0475\cdot \ln(C)$$

$$c_4 = -2.05 + 1.25\cdot T + 0.0387\cdot C - 0.00437\cdot C\cdot T$$

The current efficiency fit model provides necessary parametric representation of η function that is necessary for definition of material removal (see 2) and therefore for the full multiphysics model development. Additionally, a selection of the samples was used to measure their surface profiles, which were later utilize to validate ECM multiphysics model.

6. Multiphysics simulation results and discussion

ECM multiphysics model was developed for the experimental flow channel cell process configuration using current efficiency function (equation 10). The flow domain where the process takes place is in rectangular shape of non-scaled real dimensions. Simulation was run in transient mode after initial solution of the static model. The number of elements of 1830 was providing satisfactory results resolution. A Spooles solver was used with COMSOL default settings. Constants used in the model are gathered in Table 1. The boundary conditions are applied similar to figure 2, except that the inflow and outflow region are omitted.

Table 1. Parameters used in the COMSOL multiphysics model

Constant	Value
Gas diffusion constant D_0	1e-6 m/s^2
Faraday's constant F	96485 C/mol
Brugeman's coefficient bp	1.33
Specific heat electrolyte C_p	4200 J/(K·kg)
Thermal conductivity electrolyte h	0.6 W/(m·K)
Electrolyte viscosity η_{el}	0.001 Pa·s
Electrochemical coefficient k	2.59e-7 kg/C

Figure 5 shows a simulation with the following process parameters: C = 230 g/l, T = 10 °C, J = 53.2 A/cm^2, charge Q = 61.7 C and process time = 2.94 s. The source of temperature increase is the Joule heating. At the centre, according to the flow profile, flow velocity is maximum and convective heat flux is the highest and able to remove the heat and therefore temperature increase is minimal. At the edges flow velocity is the slowest (at the wall boundary it is 0), therefore convective flux is not able to remove the heat. Instead, conduction through the boundary enables heat transfer but conduction proceeds slower than convection and temperature increase at the walls is the highest. Additionally temperature increases cumulatively with the length of the walls where the electric potential is applied. Similar to the temperature, gas generated mainly at the cathode is also cumulated downstream the gap and gas fraction is mainly built up in the areas adjacent to the walls where flow convective flux was the smallest.

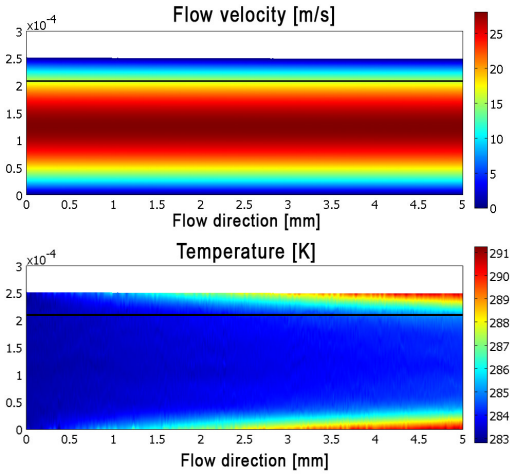

Figure 5. Results of simulation at t = 2.94 s, showing flow velocity (m/s) and the electrolyte temperature (°C) in a deformed mesh.

Figure 6 shows current density distribution and gas and temperature distributions in a greater detail at the surface of the workpiece. Current density decreases downstream as a result of the conductivity drop which is caused by predominant effect of gas generation over the temperature increase downstream the sample. The increase of temperature results in a decrease of the efficiency η and material removed is not even along the sample (Figure 7). Figure 7 shows depth of material removed predicted by simulation compared to a processed sample. Simulated depth of material removed is a reverse reflection of current density distribution alongside the sample. In reality, sample profile

differs mostly in the left side end. This is most likely due to more predominant effect of temperature on the electrolyte conductivity in reality than in the simulation model. Secondly, observed discrepancy can be caused by inaccuracies of the current efficiency fit.

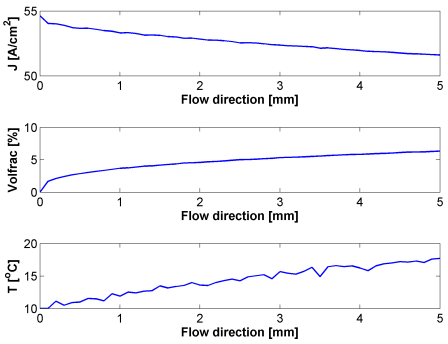

Figure 6. Distribution of the ECM process variables for t = 2.94 s.

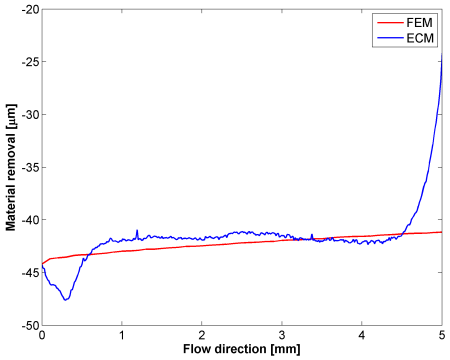

Figure 7. Experimental (blue) and simulated (red) depth of the removed material.

Developed ECM process simulation model for the flow channel cell was also deployed to predict the shape of the shaving cap. An axial symmetric model mode was used allowing downscaling simulated problem to a symmetric half of the geometry. The shaving cap was the workpiece which bottom surface was dissolved by the pre-shaped electrode (Figure 8). The 2D ECM simulation model was enhanced by a separate 3D elastic deformation simulation model. Electrolyte pressure distribution during material dissolution was used as an input for simulation of material deformation.

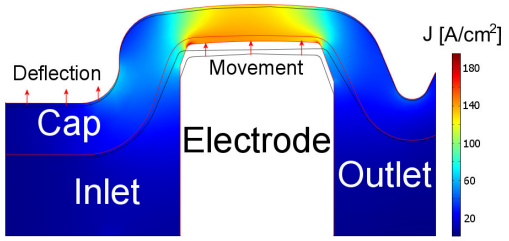

Figure 8. Axial symmetric Philips Arcitec shaving cap geometry (black line) and elastically deformed and dissolved shaving cap geometry (red line). The colour shows the current density J distribution.

This simulation allows to observe elastic deformation of the shaving cap that is progressing during material dissolution due to constant change of the product stiffness. As it can be seen in Figure 8, the centre (left) of the shaving cap is deflected due to the pressures of the process. This result enables to predict product behavior during the process in the early development stage, control or redesign the process and therefore reduce development time. ECM COMSOL simulation model can be also used for process optimization.

Presented ECM model is able to predict the ECM process phenomena qualitatively correct and with satisfactory quantitative accuracy. However, due to process complexity and complexity of simulated geometries, the model's accuracy is insufficient. This is caused by the number of simplifying assumptions that had to taken into account to compromise simulation ability and robustness. For example, one of the phenomena that are not taken into account is a difficult to describe process of salt layer build-up on the workpiece surface that affects current efficiency downstream. This phenomenon is more profound for higher than for lower electrolyte concentrations and also depends on the location on the sample affecting current efficiency. In the end, simulation results neglecting abovementioned effect elucidate 5-15% discrepancies when compared with experimental results.

Secondly, the effects of gas and temperature influence on electrolyte conductivity deviate from theoretical description in many practical cases, particularly for complex geometries like shaving cap. There are number of reasons of these deviations such as local pressure gradients, flow eddies or cavitation that are recognized but

not easy to describe in the model and therefore are not incorporated.

7. Summary

The ECM process is complex and difficult to control. Developed COMSOL model assists in process understanding, control and design. Presented simulation example has been experimentally validated and shows better agreement with the reality for higher electrolyte concentrations when the effect of gas generation is more profound and the effect of salt layer build-up is less profound. For lower electrolyte concentrations model would require further improvements. However, for the process design abovementioned inaccuracies are of the secondary importance and the COMSOL ECM model is well able to design process virtually.

8. References

1. Pajak, P.T., Investigation of Laser Assisted Electrochemical Machining, PhD Thesis, Glasgow Caledonian University, Glasgow, 2006, p1-10.
2. McGeough J.A., Advanced Methods of Maching, Chapman and Hall Ltd., London & New York, 1988, p55-87.
3. De Barr A.E. and Oliver D.A., Electrochemical Machining Unwin Brothers Ltd., Surrey, England 1975.
4. Masuzawa T. and Takawashi T., Recent Trends in ED/ECM Technologies in Japan, XIIth Int. Sym. on Electromaching (ISEM XII), Aachen, 1998, p1-15.
5. Rajurkar K.P., Zhu D., McGeough J.A., Kozak J. and De Silva A.K.M., New Developments in Electro-Chemical Maching, Annals of the CIRP, **48/2**, 1999, p1-13.
6. McGeough J.A., Principles of Electrochemical Machining, Chapman and Hall Ltd., London 1974.
7. Lubkowski K. and Kozak J., The Critical Conditions and Reliability Problems of the ECM process, ISEM XII, Aachen, 1998, p533-542.
8. Altena HS.J., Precision ECM by Process Characteristics Modelling, PhD Thesis, Glasgow Caledonian University, Glasgow, 2000, p79-140.
9. Datta M. and Landolt D., J. Electrochemical Soc. Electrochemical Science and Technology **124**, 1977, 483.
10. Datta M. and Landolt D., Acta Electrochemica **25**, 1980, 1263.

9. Acknowledgements

We would like to thank Dr. W. Hoogsteen for his contribution in the experimental research and consultancy and Mr. P.J. Huizenga for his research work on this subject during his external traineeship.